# Contrastive Credibility Propagation for Reliable Semi-Supervised Learning

Brody Kutt <sup>1</sup> Pamela Toman <sup>1</sup> Xavier Mignot <sup>1</sup> Sujit Rokka Chhetri <sup>1</sup> Shan Huang <sup>1</sup> Nandini Ramanan <sup>1</sup> Min Du <sup>1</sup> William Hewlett <sup>1</sup>

# **Abstract**

Inferencing unlabeled data from labeled data is an error-prone process. Conventional neural network training is highly sensitive to supervision errors. These two realities make semi-supervised learning (SSL) troublesome. In practice, SSL approaches often fail to outperform their fully supervised baseline. Proposed is a novel framework for deep SSL via transductive pseudo-label refinement called Contrastive Credibility Propagation (CCP). Through an iterative process of refining soft pseudo-labels, CCP unifies a novel contrastive approach for generating pseudo-labels and a powerful technique to overcome instancedependent label noise. The result is an SSL classification framework explicitly designed to overcome inevitable pseudo-label errors. Using standard text and image benchmark classification datasets, we show CCP reliably boosts or matches performance over a supervised baseline in four common real-world SSL scenarios: fewlabel, open-set, noisy-label, and class distribution misalignment.

### 1. Introduction

Leveraging massive datasets that are only partially labeled is critical for countless applications (Wang et al., 2020; Zhou et al., 2022; Ding et al., 2022; de Carvalho et al., 2022; Gao et al., 2022; Liu et al., 2022; Lugo et al., 2022). Generating and utilizing pseudo-labels for unlabeled data is a powerful but error-prone approach. Common issues often challenge the resulting classifier's ability to reliably perform better than a fully supervised baseline (Oliver et al., 2018). Some of these issues, illustrated in Fig. 1, and how our work addresses them, are described below.

**A)** Error propagation: An incorrect pseudo-label can cause a cascade of future errors. In the original label propa-

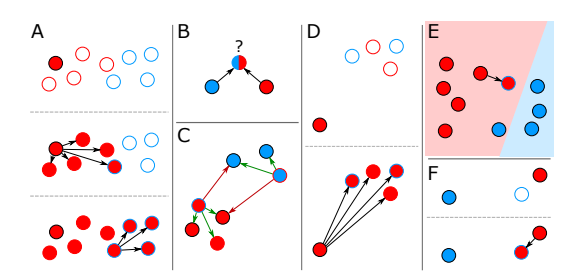


Figure 1: Six common issues of pseudo-labeling algorithms. The color of the interior of each circle indicates the predicted class. The outline of each circle indicates the true class and black outlines indicate a labeled sample. Black arrows indicate label propagation influence. In C, repulsive (dark red) and attractive (green) arrows indicate gradient influence. In E, the background color indicates a decision surface.

gation algorithm (LPA) (Zhu & Ghahramani, 2002), upon which several more recent techniques are based (Malhotra & Chug, 2021; Xie et al., 2011; Li et al., 2021a; Chin & Ratnavelu, 2017; Li et al., 2020; Dong et al., 2020), label information iteratively diffuses across unlabeled samples whether the initial propagation is correct or not. Our approach eliminates error propagation at the batch level by focusing exclusively on first-order, *i.e.* single-hop, similarities. High-order propagation is made possible through multiple iterations of Algorithm 1.

**B)** Ambiguity: The true class of unlabeled samples is sometimes unknowable e.g. if it is highly similar to two different classes. In a similar fashion to (Dong et al., 2020), our approach uses what we call credibility vectors (see Sec. 3.1), as opposed to traditional label vectors, to help reflect low prediction weight in this scenario. The output credibility vector for such a sample,  $q_i$ , will feature near-zero scores for the equally similar classes and < 0 scores for every other class.  $q_i$  values of  $\le 0$  induce no effect throughout the framework and near-zero values induce a minimal effect. In general, credibility adjustments help softly differentiate uncontested estimated similarities by giving them higher weight.

<sup>&</sup>lt;sup>1</sup>AI Research, Palo Alto Networks, Santa Clara, CA. Correspondence to: Brody Kutt <a href="mailto:bkutt@paloaltonetworks.com">bkutt <a href="mailto:bkutt@paloaltonetworks.com">bkutt <a href="mailto:bkutt@paloaltonetworks.com">bkutt <a href="mailto:bkutt@paloaltonetworks.com">bkutt <a href="mailto:bkutt@paloaltonetworks.com">bkutt <a href="mailto:bkutt@paloaltonetworks.com">bkutt@paloaltonetworks.com</a>>.

C) Inappropriate similarity metrics: Learned similarity metrics for SSL often suffer from confirmation bias (Arazo et al., 2020). This occurs when a network is optimized to produce similarities corresponding to its label predictions. To combat confirmation bias, the noisy results of the propagation mechanism (Algorithm 2) do not affect our loss during the pseudo-label assignment. A single CCP iteration consists of many epochs while minimizing our Soft Supervised Contrastive (SSC) loss (denoted  $\mathcal{L}_{SSC}$ ) which is a generalization of Supervised Contrastive (SupCon) loss (Khosla et al., 2020) and its self-supervised counterpart, SimCLR loss (Chen et al., 2020a;b). Only after the iteration has concluded do we update our soft pseudo-labels by averaging all predictions across epochs. Averaged predictions capture network oscillations and inconsistencies across batches. Unlabeled samples influence  $\mathcal{L}_{SSC}$  and Algorithm 2 only via their averaged pseudo-labels. This process, CCP's outermost iteration, is modeled after an algorithm developed to correct instance-dependent label noise called SEAL (Chen et al., 2021). We find incorrect pseudo-labels correct themselves across iterations in a similar fashion (Appendix **C**).

**D)** Forced propagation: Pseudo-labels are often forced to carry a certain total weight, usually through the use of a softmax function (Chen et al., 2022). This eliminates a propagation mechanism's ability to abstain from prediction even if the similarity to all classes is weak. Adjacency matrix row normalization in graph-based label propagation produces the same effect (Zhu & Ghahramani, 2002; Kamnitsas et al., 2018). In Algorithm 2, class similarities are all computed independently. Credibility adjustments do not enforce the pseudo-label to sum to any specific value. An unlabeled sample that has near-zero similarity to all classes will have a credibility vector of near-zero values. Through the use of weighted arithmetic means in  $\mathcal{L}_{SSC}$  and Algorithm 2, as well as a weighted classification loss, these samples will have minimal influence on the framework. This is especially relevant in the presence of unlabeled data that belongs to no class (called open-set SSL) which can cripple existing approaches (Oliver et al., 2018). The ability to abstain from prediction enables CCP to safely leverage all pseudo-labels instead of simply discarding a percentage of the weakest pseudo-labels as is common practice (Sohn et al., 2020; Li et al., 2021b; Zheng et al., 2022).

E) Classification sensitivity to label errors: Deep learning classifiers with conventional cross-entropy loss are sensitive to label errors (Song et al., 2020). Classifiers often directly influence pseudo-label generation while simultaneously learning from noisy pseudo-labels (Yang et al., 2021; Lee et al., 2013; Zheng et al., 2022) which can cause an error cascade. Recent work has explored why contrastive representations boost robustness to label noise (Ghosh &

Lan, 2021). In our approach, only softly supervised contrastive representations are used for pseudo-label generation. Further, subsampling pseudo-labels between iterations and after the conclusion of CCP eliminates many erroneous or weakly predicted samples. We propose an unsupervised, principled subsampling approach in Sec. 3.3.

F) Propagation sensitivity to similarity metrics: Pseudo-label accuracy is often at the mercy of your similarity metric. Similar to (Berthelot et al., 2019b), our approach averages predicted credibility vectors across transformed views of data for increased error resistance. Unlike other work, if two different predictions occur for two transformed views of a sample, even when each has high confidence, the average *credibility-adjusted* pseudo-label will consist of all near-zero values. Unlike (Berthelot et al., 2019b), no sharpening takes place on the average vector to prevent forcing a pseudo-label with weak evidence.

The evaluation of SSL algorithms often only explores the few-label learning scenario i.e. balanced reduction of the number of given labels. Our work expands upon this with three other common real-world SSL scenarios. These are open-set (some unlabeled data belongs to no class), noisylabel (some of the given labels are incorrect), and class distribution misalignment (labeled and unlabeled data have different class frequency distributions). Our contributions are as follows. To the best of our knowledge, CCP is the first SSL algorithm to 1) Make use of credibility vectors as we define them to properly represent uncertainty. 2) Imbue a pseudo-labeling strategy with an approach to overcome instance-dependent label noise. 3) Introduce a generalizable, unsupervised strategy to choose a dynamic pseudo-label subsampling rate. 4) Demonstrate a reliable performance boost over a supervised baseline in four real-world SSL data scenarios with a single solution.

# 2. Related Work

SSL has a rich history in AI research (Yang et al., 2021; Chapelle et al., 2006). We focus on two dominant approaches. These are pseudo-labeling and consistency training. CCP draws inspiration from both approaches.

**Pseudo-labeling:** These methods typically constitute transductive learning (Shi et al., 2018; Iscen et al., 2019). Here, the objective is to generate proxy labels for unlabeled instances, *e.g.* via transductive inference, to enhance the learning of an inductive model. Seminal work (Lee et al., 2013) simply uses the classifier in training to produce pseudo-labels which are trained upon directly. This is problematic in that it actively promotes confirmation bias and it heavily relies on the fitness of the pseudo-labels. This was later extended to include a measure of confidence of

pseudo-labels in (Shi et al., 2018). Closely related is the concept of self-training which iteratively integrates into training the most confident pseudo-labeled samples and repeats (Dong & Schäfer, 2011; Sahito et al., 2021; Xie et al., 2020b). These techniques are sometimes unstable when pseudo-label error accumulates across iterations. More recent work has tried to address accumulating errors by using independent models for utilizing pseudo-labels (Chen et al., 2022). As mentioned previously, LPA (Zhu & Ghahramani, 2002) is a popular graph-based technique for generating pseudo-labels but has many failure cases (Dong et al., 2020). Much work tends to use LPA as a transductive inference mechanism. Such inferred pseudo-labels are highly noisy and thus problematic for SSL. Work in (Kamnitsas et al., 2018) tries to circumvent this by instead using LPA-derived pseudo-labels only for graph-based regularization of the encoder. Like CCP, (Wang & Wu, 2022) proposed repeatedly re-predicting pseudo-labels during an optimization framework akin to self-training. Although there has been much success in employing previous pseudo-labeling-based SSL approaches, they tend to break down when faced with highly unreliable pseudo-labels.

Consistency Training: Analogous to perturbation-based SSL and contrastive learning, these techniques train a network to produce a single, distinct output for a sample under different augmentations (transformations). Work in (Xie et al., 2020a) minimizes a consistency loss for unlabeled data and a standard classification loss simultaneously which could introduce irreconcilable gradients. Other work (Chen et al., 2020a;b), shown superior to (Xie et al., 2020a) in SSL, employ an unsupervised consistency-like loss in a pretraining stage before training solely with clean labels. Unsupervised consistency loss is attractive in that it eliminates supervision errors but lacks power in that class structure from unlabeled data is never leveraged directly. Instead, CCP introduces a softly supervised consistency (contrastive) loss with true and pseudo-labels.

# 3. Contrastive Credibility Propagation (CCP)

Here we present our proposed method for transductive pseudo-label refinement called Contrastive Credibility Propagation (CCP). We establish notation, introduce credibility vectors, describe the CCP iteration, introduce our subsampling procedure, formalize our loss functions, then explain how to build a classifier on CCP pseudo-labels.

Consider a classification task among a set of K classes  $c = [0, 1, \ldots, K-1]$ . Consider a dataset  $X = \{x_0, \ldots, x_{N-1}\}$  of N samples. Denote indices to labeled (unlabeled) samples as L (U). Each labeled sample  $l \in L$  has a known one-hot class vector  $y_l \in [0, 1]^K$  with a 1 (0) in the on (off) position. We maintain a real-valued credibility vector  $q_i$  of

length K for each sample  $i: q_i \in [-1, 1]^K$  (see Sec. 3.1). In training, denote the indices of a random batch of size n as  $\mathcal{B} \subseteq L \cup U$ . We define a set of data transformations,  $\mathcal{T}$ . We draw two transformations,  $t_1, t_2 \in \mathcal{T}$ , randomly for every batch. A transformed pair will share one  $q_i$ . Thus, a batch of transformed data and credibility vector tuples will be of size 2n denoted  $\{(x_i^{t_1}, q_i), (x_i^{t_2}, q_i)\}_{i \in \mathcal{B}}$ . An encoder  $f_b$ , computes a vector encoding  $f_b(x) = b$ . One projection head  $f_z$  computes a vector encoding used for contrastive learning,  $f_z(b) = z$ . A separate projection head,  $f_q$ , computes  $f_q(b) = g \in \mathbb{R}^K$  with which we apply a classification loss.  $f_a$  and  $f_z$  consist of a nonlinear MLP. We reset  $f_b$  and  $f_z$  between iterations of CCP to learn new representations. Attaching  $f_g$  and  $f_z$  to  $f_b$  is motivated by prior work (Chen et al., 2020a;b; Khosla et al., 2020). An illustration of these components is provided in Appendix A. We minimize a softly supervised contrastive loss while we are performing CCP (Algorithm 1). The conclusion of CCP provides soft labels (credibility vectors) for all unlabeled data which are then used to build a classifier.

The similarity function we use throughout this work is angular similarity, motivated by prior work (Chen et al., 2020a; Cer et al., 2018). Similarities are computed solely upon z vectors produced by the projection head  $f_z$ . Angular similarity is defined by  $\phi(z_i, z_j) = 1 - \arccos\left(\frac{z_i \cdot z_j}{\|z_i\| \|z_i\|}\right) / \pi$ .

#### 3.1. Credibility Adjustments

The CCP algorithm iteratively assigns and refines credibility vectors to all unlabeled samples,  $\{q_u\}_{u\in U}$ . A credibility vector is a vector that represents the confidence of a sample belonging to a certain class. Unlike probability vectors, credibility vectors do not sum to 1. Credibility vectors are more expressive than one-hot label vectors. A credibility score of 1 means maximum confidence in class membership, 0 means uncertainty and -1 means maximum confidence in class non-membership. Verbally, a credibility score for a sample and class is the similarity between that sample and class minus the highest similarity to all other classes. Credibility adjustments are formalized in Algorithm 1, Lines 15 to 17 and Algorithm 2, Lines 7 to 9. The core idea of credibility, similar to (Dong et al., 2020), is to extend similarity measurements to capture ambiguity brought forth by competing similarities. For trusted labeled data, credibility vectors,  $\{q_l\}_{l\in L}$ , are clamped with 1 (0) in the on (off) position. When we apply credibility vectors to  $\mathcal{L}_{SSC}$ ,  $\mathcal{L}_{CLS}$ , and Algorithm 2, we clip credibility vectors to a range of [0, 1]. A clipped credibility vector consists of zeros everywhere except the strongest class which is scaled down by the second strongest class value. Negative values of credibility vectors produced in a batch are still useful when averaging across epochs in Line 14. Note that  $\mathcal{L}_{SSC}$  and Algorithm 2 feature weighted averages. The weights are derived directly from the values of the associated  $q_i$ 's.  $\mathcal{L}_{CLS}$  is scaled by

the magnitude of values in  $q_i$ . At initialization, unlabeled data receive  $q_i = \vec{0}$  to ensure they do not influence either. A concrete example of credibility adjustments and how it compares to traditional label vectors in a cross-entropy calculation is shown in Append A.

#### 3.2. The CCP Iteration

During a single iteration of CCP (Algorithm 1), we predict a credibility vector for every unlabeled sample  $\Xi$  times while simultaneously minimizing a soft supervised contrastive loss,  $\mathcal{L}_{SSC}$ . We store all credibility vectors for unlabeled samples and then average them together at the end of the iteration. The SEAL algorithm (Chen et al., 2021), which bears similarity to CCP's outermost iteration (Line 6), is designed to correct the label of mislabeled samples in fully supervised problems. It was found that, during training, network predictions frequently oscillate between incorrect and correct labels in the presence of label noise. This suggests averaging the predictions made across epochs to correct label noise. Similarly, propagated pseudo-labels are subjected to the randomness of the instantaneous network state and batch selection. Concretely, in the presence of pseudo-label error, we observe the same oscillatory behavior reported in (Chen et al., 2021) of the predicted pseudo-label. This enables a similar theoretical intuition behind epoch averaging.

$$\|\mathbb{E}[q_u^{[m+1]}] - q_u^*\| \le \|q_u^{[m]} - q_u^*\| \tag{1}$$

Where  $\|\cdot\|$  is a vector norm,  $q_u^{[m]} \in \mathbb{R}^K$  is the pseudolabel of sample u at iteration m, and  $q_u^* \in \mathbb{R}^K$  is the latent optimal pseudo-label of sample u. Namely, incorrect pseudo-labels gradually move to their optimal state across CCP iterations. Refer to Appendix H for the derivation of Eq. (1) and plots depicting oscillatory pseudo-label behavior. Furthermore, the choice to model our outermost iteration after SEAL is due to it combating instance-dependent instead of class-conditional label noise. The "label noise" we are trying to overcome in CCP arrives via transduction and is thus strongly instance-dependent. The value of  $\Xi$ should be sufficient to see proper convergence of  $\mathcal{L}_{SSC}$ . The initial values for  $f_b$  and  $f_z$  at Line 5 can be defined randomly or via self-supervised pretraining. Pretraining with  $\mathcal{L}_{SSC}$ 's self-supervised special case, SimCLR loss, often greatly improves pseudo-label accuracy, especially in a fewlabel scenario. In Line 7, every batch can contain labeled (unlabeled) samples with indices  $\mathcal{B}_l \subseteq L$  ( $\mathcal{B}_u \subseteq U$ ). Ensuring both are present is important in the first iteration of CCP when unlabeled data has no pseudo-label. After the first iteration, purely random batch sampling can be used. Within a transformed batch of samples and credibility vectors,  $\{(x_i^{t_1}, q_i), (x_i^{t_2}, q_i)\}_{i \in \mathcal{B}}$ , credibility vectors will be generated for each of an unlabeled transformed pair independently,  $\{\tilde{q}_u^{t_1}, \tilde{q}_u^{t_2}\}_{u \in \mathcal{B}_u}$ . We then compute a single predicted

credibility vector for a transformed pair by averaging them together (Algorithm 2, Line 11). In addition to error resistance, we can transform out of the labeled distribution to propagate labeled information to a wider scope without introducing label errors.

```
Algorithm 1 An iteration of the CCP algorithm.
```

```
1: Given \Xi, \mathcal{T}, \{q_l\}_{l\in L}, X, p_{\text{last}}, d_{\text{max}}
  2: if \{q_u\}_{u\in U} are not available then
             Initialize q_u = \vec{0} for u \in U
  3:
  4: end if
  5: Reset network variables in f_b, f_z
  6: for \xi \in \{1, 2, \dots, \Xi\} do
             for semi-labeled batches \{(x_i, q_i)\}_{i \in \mathcal{B}_l \cup \mathcal{B}_u} do
  7:
                   Randomly draw t_1, t_2 \in \mathcal{T} to form
      f_z(f_b(x_i^{t_2}))) for i \in \mathcal{B}_l \cup \mathcal{B}_n
        \begin{array}{c} \text{Compute } \{\tilde{q}_j^{[\xi]}\}_{j\in\mathcal{B}_u} \text{ using Algorithm 2} \\ \text{Train } f_b, \ f_z \text{ using the gradient of } \mathcal{L}_{\text{SSC}} \text{ computed with } \{(z_t^{t_1}, q_i), (z_t^{t_2}, q_i))\}_{i\in\mathcal{B}_l\cup\mathcal{B}_u} \end{array}
10:
11:
12:
13: end for
14: Update \hat{q}_u=\frac{1}{\gamma}\sum_{\xi=1}^{\Xi}\tilde{q}_u^{[\xi]}/\Xi for u\in U 15: for k\in c do
             q_{u,k} = \hat{q}_{u,k} - \max_{k' \in c \setminus k} (\hat{q}_{u,k'}) \text{ for } u \in U
16:
17: end for
18: Clip all values in \{q_u\}_{u\in U} to lie in [0,1]
19: Compute p, \{\hat{\omega}_u\}_{u\in U} using Algorithm 3
20: Set the bottom p\% of \{q_u\}_{u\in U} to \vec{0} ordered by
21: Update p_{\text{last}} = p, d_{\text{max}} = d_{\text{max}}/10
22: Return f_b, p_{last}, d_{max}, \{q_u\}_{u \in U} (used in next iteration)
```

In Algorithm 1, Lines 14 to 18, we adjust  $\{\hat{q}_u\}_{u\in U}$  in several ways to make them more suitable as labels. In Line 14, we include a scaling factor  $^1\!/\gamma$  outside the average to scale the strength of credibility vectors. Our choice for  $\gamma$  is the value of the maximum strength among all averaged pseudolabels,  $\gamma = \max_{u\in U, c\in K} \sum_{\xi=1}^{\Xi} \tilde{q}_{u,c}^{(\xi)}/\Xi$ . This ensures the strongest pseudo-label will have a strength of 1. Before we clip all values outside the range of [0,1] in Line 18, we compute a final credibility adjustment on every vector to ensure that the final pseudo-label is a proper credibility representation. The scaled, credibility adjusted, and clipped vectors are denoted  $\{q_u\}_{u\in U}$ .

#### 3.3. Subsampling

In Line 19, we use Algorithm 3 to decide which predictions to subsample. This is inspired by self-training mechanisms (Amini et al., 2022). These techniques typically use the max score of a learned classifier as an indicator

## Algorithm 2 Compute propagated credibility vectors.

```
1: Given \{(z_i^{t_1}, q_i), (z_i^{t_2}, q_i)\}_{i \in \mathcal{B}_l \cup \mathcal{B}_u}
  2: for j \in \mathcal{B}_u do
                 for t \in \{t_1, t_2\} do
  3:
                         for k \in c do
  4:
                                  \psi_{j,k}^{t} = \frac{\sum_{i \in \mathcal{B} \setminus j} \phi(z_{j}^{t}, z_{i}^{t_{1}}) q_{i,k} + \phi(z_{j}^{t}, z_{i}^{t_{2}}) q_{i,k}}{2 \sum_{i \in \mathcal{B} \setminus i} q_{i,k}}
  5:
  6:
                         \tilde{q}_{j,k}^t = \psi_{j,k} - \max_{k' \in c \backslash k} (\psi_{j,k'}) end for
                          for k \in c do
  7:
  8:
  9:
                 end for
10:
                 Store \tilde{q}_j = \frac{\tilde{q}_j^{t_1} + \tilde{q}_j^{t_2}}{2}
11:
12: end for
13: Return \{\tilde{q}_j\}_{j\in\mathcal{B}_u}
```

of confidence. Similarly, our indicator of confidence for a credibility vector is the maximum of its unclipped values, i.e.  $\{\hat{\omega}_u = \max(\hat{q}_u)\}_{u \in U}$ . The credibility vectors with the lowest confidence are "reset" back to the zero vector between iterations of CCP or discarded when building a classifier. During pseudo-label assignment, this allows CCP to iteratively build up a picture of the class structure contained in unlabeled data using "easy" unlabeled samples to later predict "hard" ones. We compute a percentage  $p \in \{0\%, 1\%, \dots, 99\%\}$  that represents what percent of least confident  $\{q_u\}_{u\in U}$  will be reset or discarded. Performance gains can be achieved from careful subsampling (Appendix C). However, aggressive p values can derail CCP effectiveness. We hypothesize the instability is similar in cause to the instability of self-training mechanisms (Sohn et al., 2020). Unlike self-training, CCP is shown highly stable without any subsampling. Accordingly, our approach is to balance the desire of resetting weak vectors with limiting the divergence of the predicted class distribution of the selected unlabeled data from the predicted class distribution of all unlabeled data. Importantly, unlike other work (Wang et al., 2019; Berthelot et al., 2019a; Oh et al., 2021; Zheng et al., 2022), we leverage no assumptions about the true class frequency distribution of unlabeled data. We argue that such assumptions, e.g. the use of distribution alignment (aligning the marginal distribution of predicted labels with ground-truth labels), are rarely applicable to real-world datasets where unlabeled data may assume any distribution.

Concretely, in Algorithm 3, Line 3 we compute the anchor distribution, Q, by summing the weights for every class across all  $\{q_u\}_{u\in U}$  and dividing by the total mass. We search over candidate p's with one minus the p used in the previous iteration,  $p_{\text{last}}-1\%$ , as the maximum to ensure we don't increase p between iterations. At Line 6, we compute the new distribution, P, obtained after resetting the

candidate percentage of vectors. At Line 7, we compute the Kullback–Leibler (KL) divergence (Csiszar, 1975) between these distributions. At Line 9, we choose p by selecting the maximum candidate that obeys a strict limit on the divergence,  $d_{\rm max}$ . Also to support convergence, we divide  $d_{\rm max}$  by 10 for the next iteration. In summary, this algorithm aims to subsample the data such that the class distribution of the subsampled data is as close as possible to the original data. Our metric is unsupervised, free of imposing assumptions and normalized with respect to the dataset size. This suggests, in theory, a single schedule for  $d_{\rm max}$  should generalize well across datasets. Indeed, in practice, we find an initial value of  $d_{\rm max}=0.01$  to work *generally* well across all our benchmark datasets between iterations of CCP and when building a classifier (see Appendix C).

## Algorithm 3 Compute a subsample percentage.

```
1: Given \{\hat{q}_u\}_{u \in U}, \{q_u\}_{u \in U}, p_{\text{last}}, d_{\text{max}}

2: Compute \{\hat{\omega}_u = \max(\hat{q}_u)\}_{u \in U}

3: Q = \sum_u^U q_u / \sum_k^c \sum_u^U q_{u,k}

4: for p_i \in \{0\%, 1\%, \dots, p_{\text{last}} - 1\%\} do

5: Set the bottom p_i\% of \{q_u\}_{u \in U} to \vec{0} ordered by \{\hat{\omega}_u\}_{u \in U}

6: P = \sum_u^U q_u / \sum_k^c \sum_u^U q_{u,k}

7: d_i = D_{\text{KL}}(P \parallel Q) = \sum_{k \in c} P_k \log_2{(P_k/Q_k)}

8: end for

9: p = \max(\{p_i \text{ for all } i \text{ such that } d_i < d_{\text{max}}\})

10: Return p, \{\hat{\omega}_u\}_{u \in U}
```

### 3.4. Soft Loss Functions

 $\mathcal{L}_{\text{SSC}}$  and  $\mathcal{L}_{\text{CLS}}$  are fully supervised loss functions that utilize  $\{q_u\}_{u\in U}$  provided by the CCP algorithm. Algorithm 2, which is inevitably error-prone at the batch level, is functionally isolated from the error-sensitive mechanisms for supervised contrastive and classification learning. Transformed pairs are not treated uniquely in  $\mathcal{L}_{\text{SSC}}$  or  $\mathcal{L}_{\text{CLS}}$ . In other words, transformed pairs can be considered independent samples with identical credibility vectors. To simplify the notation, we formalize  $\mathcal{L}_{\text{SSC}}$  and  $\mathcal{L}_{\text{CLS}}$  for an arbitrary batch of data and (clipped) credibility vector tuples,  $\{(x_i, q_i)\}_{i\in\mathcal{B}}$ .

We define an  $n\times n$  pairwise matching matrix, M, where  $m_{i,j}=q_i\cdot q_j$  for  $i,j\in\mathcal{B}$ . Each row of M contains the weights of a weighted arithmetic mean of normalized losses for that sample to all other samples based on the evidence of a positive pair relationship. We scale pairwise similarities by temperature  $\tau$  and take the exponential as in prior work (Chen et al., 2020a;b; Khosla et al., 2020) to form a  $n\times n$  matrix A defined by  $a_{i,j}=\exp(\phi(z_i,z_j)/\tau)$  for  $i,j\in\mathcal{B}$ . We construct a strength vector,  $\omega$ , defined by  $\omega_i=\max(q_i)$  for  $i\in\mathcal{B}$ . Each  $\omega_i$  contains the confidence of  $q_i$ . It serves to scale the magnitude of loss on sample i and the corresponding entries in the normalizing factor for each

 $a_{i,j}$ . We ignore comparisons of the same sample with the following modifications  $M=M\odot(1-\mathbb{I}), A=A\odot(1-\mathbb{I})$  where  $\odot$  is element-wise multiplication. We can now define  $\mathcal{L}_{\rm SSC}$  defined over  $\mathcal{B}$ ,

$$\mathcal{L}_{SSC} = -\frac{1}{n} \sum_{i \in \mathcal{B}} \frac{\omega_i}{\sum m_i} \sum_{j \in \mathcal{B}} m_{i,j} \log \left( \frac{a_{i,j}}{a_i \cdot \omega} \right)$$
 (2)

SimCLR and SupCon loss are special cases of  $\mathcal{L}_{SSC}$ . In  $\mathcal{L}_{SSC}$ , positive pairs are not specified discretely. Every pair of samples has a score in M between 0 and 1 which corresponds to how much evidence there is that they constitute a positive pair. If all data is labeled with maximum confidence,  $\mathcal{L}_{SSC}$  becomes SupCon loss. If all data is unlabeled, only transformed pairs have a maximum positive pair relationship, and all  $\omega_i = 1$ ,  $\mathcal{L}_{SSC}$  becomes SimCLR loss. Circumventing the discrete selection of positive pairs better reflects the true state of pseudo-labels e.g. compared to (Zhang et al., 2022).

When training a classifier, we use a cross-entropy loss that is similar to SEAL loss except that we feed in  $q_i$  in place of normal label vectors. We use the output from  $f_g$  instead of  $f_z$ . We send each  $g_i$  through a softmax,  $\sigma(g_i)$ ,

$$\mathcal{L}_{CLS} = -\frac{1}{n} \sum_{i \in \mathcal{B}} \sum_{k \in c} q_{i,k} \log \left( \sigma(g_i)_k \right)$$
 (3)

Note that because  $q_i$  is not a probability distribution,  $\mathcal{L}_{\text{CLS}}$  does not strictly compute a cross-entropy. However, the gradient remains the same. One can interpret  $\mathcal{L}_{\text{CLS}}$  as a credibility-weighted version of categorical cross-entropy. Recall each  $q_i$  will contain only one non-zero entry. Assume this non-zero entry is index k. The value of  $\mathcal{L}_{\text{CLS}}$  for sample i can be written as  $\omega_i \log (\sigma(g_i)_k)$ .

# 3.5. Building a Classifier

After CCP has concluded, we apply the soft labels,  $\{q_u\}_{u\in U}$ , with a classification loss described in Eq. (3). We can reuse the final state of  $f_b$  as a pretrained initialization when we train our classifier head,  $f_g$ , to speed up convergence. However, your pretrained  $f_b$  will not be built on the latest pseudolabels computed at the end of the final CCP iteration. In our experiments, resetting  $f_b$  (to a random state or a self-supervised pretrained state) after the final iteration of CCP is more effective. We can also tune  $d_{\max}$  in Algorithm 3 to subsample the final  $\{q_u\}_{u\in U}$ . The vectors we eliminate will simply be discarded as opposed to being reset to  $\vec{0}$ .

# 4. Experimental Results

As explained in Sec. 1, our experiments focus on testing the reliability of CCP to outperform a supervised baseline in

four common SSL data scenarios. We also compare CCP to other SSL algorithms where applicable. In our experiments, we use four well-known text classification datasets (AG News (Zhang et al., 2015), DBpedia (Zhang et al., 2015; Lehmann et al., 2014), Rotten Tomatoes (Pang & Lee, 2005), Yahoo! Answers (Chang et al., 2008; Zhang et al., 2015)) and one image classification dataset (CIFAR-10 (Krizhevsky & Hinton, 2009)). We also experimented with a dataset for data loss prevention (DLP) that we collected ourselves. A DLP classifier is designed to identify different kinds of sensitive documents and properly ignore everything else. Our dataset consists of 559,141 documents with the following class breakdown: 30,048 accounting documents, 10,795 invoices, 16,282 healthcare documents, 50,763 lawsuit documents, 5,121 patent filings, 47,741 C source code files, 53,529 Java source code files, and 344,862 non-sensitive documents like encyclopedia pages, dictionary pages, excerpts from books, news articles, chatroom transcripts, etc. Some summary information can be found about these datasets in Appendix B.

We use a common neural network solution for each of the text datasets. The solution is similar to other work that uses convolutional networks for text classification (Zhang et al., 2015; Kutt et al., 2021; Kim, 2014; Johnson & Zhang, 2015). Briefly, text data is tokenized and each token index is used to look up a corresponding embedded vector (EV). The sequence of EVs is then processed by a convolutional neural network. For image classification, we follow the setups of prior work for comparability (Oliver et al., 2018; Sohn et al., 2020; Zheng et al., 2022). For image data,  $f_b$  takes the form of a WRN28-2 (Zagoruyko & Komodakis, 2016). All CCP iterations on CIFAR-10 used self-supervised pretraining to initialize  $f_b$  and  $f_z$ . More information to recreate our experiments can be found in Appendix G.

### 4.1. Data Transformations

For text data, we design a set of transformations,  $\mathcal{T}$ , inspired by the simplest and computationally cheapest set of transformations found in (Bhattacharjee et al., 2022). All transformations are implemented as tensor operations in the computational graph. All transformations act on a sample after it has been converted to a sequence of EVs and allow a gradient to pass through them. These consist of applying Laplacian noise consistent with Differential Privacy (Dwork, 2011), applying Gaussian noise, randomly hiding and scrambling the order of EVs, and randomly swapping paragraphs and EVs. The use of transformations alone garners large accuracy increases for every algorithm particularly when label information is scarce. To eliminate this effect on our text experiments, every algorithm tested use the same  $\mathcal{T}$ (and augmented batches). For images, we repeat the transformations found in (Chen et al., 2020a) including random cropping, horizontal flipping, and color distortions. Further

details can be found in Appendix F

### 4.2. Few-Label Performance

For text data, we compare CCP to a supervised cross-entropy control with access to all labels, a supervised cross-entropy baseline, and three algorithms that bear important similarities to CCP at varying levels of label availability in Tab. 1. SimCLR loss and SupCon loss are included as they are specific cases of  $\mathcal{L}_{SSC}$ . Further, the Compact Clustering via Label Propagation (CCLP) regularizer can also be seen as a semi-supervised counterpart of SupCon. SimCLR and SupCon use the same  $f_z$  and  $f_g$  that we use with CCP. For CCLP, we attach  $f_g$  to  $f_b$  and apply CCLP to the hidden layer of  $f_q$  for a fair comparison. CCLP calls for linear decision boundaries formed after the hidden space where CCLP is applied via a traditional classification loss applied immediately after a final fully connected layer. We also search over the CCLP-specific hyperparameters such as the number of steps and CCLP weight and report the best results. All networks are trained until convergence according to their originally prescribed procedure. Each CCP experiment consists of 8 iterations. We use the same subsampling procedure (initial  $d_{\text{max}} = 0.01$ , divided by 10 after each iteration) for each experiment both between CCP iterations and after its conclusion.

% of Labels	Algorithm	DLP	AG News	DBpedia	Rotten Tomatoes	Yahoo! Answers
100%	Control	99.95%	91.95%	98.79%	82.01%	73.17%
	Baseline	99.23%	85.51%	94.25%	66.39%	63.24%
	CCLP	99.03%	79.54%	97.57%	64.48%	51.88%
1%	SimCLR	99.46%	86.89%	95.91%	68.10%	57.72%
	SupCon	99.40%	85.92%	96.12%	66.97%	60.19%
	CCP (ours)	99.70%	88.89%	98.24%	71.14%	68.26%
	Baseline	97.17%	78.37%	86.47%	59.89%	53.44%
	CCLP	95.56%	50.66%	67.24%	57.02%	37.80%
0.1%	SimCLR	97.50%	80.57%	87.75%	59.42%	37.69%
	SupCon	97.56%	74.84%	84.97%	57.96%	36.38%
	CCP (ours)	98.88%	87.04%	96.20%	60.85%	63.23%
0.05%	Baseline	94.71%	71.91%	72.71%	57.15%	48.86%
	CCLP	91.71%	50.17%	60.13%	55.53%	33.62%
	SimCLR	95.32%	77.09%	83.08%	56.07%	38.79%
	SupCon	94.96%	68.46%	80.70%	57.42%	28.25%
	CCP (ours)	96.03%	85.14%	93.84%	57.35%	59.58%

Table 1: The best test set accuracy across all text datasets.

In Tab. 1, our intention is not to demonstrate state-of-the-art performance on these datasets. A different choice of  $f_b$  would likely provide higher accuracy. In contrast, we intend to explore how CCP fares when a supervised baseline is largely unreliable. Note that only CCP is able to outperform or match the baseline in every experiment. SimCLR often outperforms the baseline, but CCP outperforms SimCLR in every experiment by the widest margin when label availability is lowest. CCLP underperforms the baseline in every experiment except on DBpedia with 1% label availability

i.e. when the baseline is highly accurate and the classes are balanced. When CCLP succeeds, it outperforms the pretraining methods likely because it makes direct use of pseudo-labels. CCLP and CCP, like many other SSL algorithms, rely on network fitness for quality pseudo-labels. Accordingly, the margin of success for CCP shrinks as the baseline becomes less accurate e.g. on Rotten Tomatoes with 0.05% label availability where the baseline is <8% better than random guessing.

For CIFAR-10, following the CCP iterations detailed in Appendix C, we found a test set classification accuracy of 84.91%, 88.82%, and 91.37% at the label availability levels of 40, 250, and 4000, respectively. Our fully supervised control accuracy is 94.78%. While not perfect, you can compare these results to what is reported in (Zheng et al., 2022), given the similar setup. At the 40 label availability level, CCP performs significantly better than prior methods like UDA (Xie et al., 2020a), MixMatch (Berthelot et al., 2019b), and ReMixMatch (Berthelot et al., 2019a) at 70.95%, 52.46%, and 80.90%, respectively. However, CCP is well below SimMatch's reported accuracy of 94.40%. SimMatch however also reports performance at the 4000 label availability level that is 1.26% above our control. Careful hyperparameter tuning and further CCP iterations may shrink that gap. Importantly, unlike SimMatch and many other modern methods, CCP achieves these results without distribution alignment, which is not a valid assumption for our other three SSL data scenarios.

## 4.3. Open-Set & Misalignment Performance

We recreate the experiment found in (Oliver et al., 2018) to simultaneously explore the open-set and misalignment data scenarios. Briefly, 400 labeled examples of classes bird, cat, deer, dog, frog, and horse are isolated. Originally, each class has 5000 labeled samples. Unlabeled data is sourced as 5000-400 = 4600 samples from each of the four classes. In the 0% mismatch scenario, these four classes are deer, dog, frog, and horse. In the 100% mismatch scenario, these four classes are airplane, automobile, ship, and truck. Mismatch percentage scenarios between these replace indistribution classes with out-of-distribution (OOD) classes one-by-one. The test set only contains in-distribution data. In Fig. 3, we can see that the test accuracy of CCP can perform strictly above or at the level of a supervised baseline at all degrees of mismatch. We ran CCP for only a single iteration and then built a classifier on the pseudo-labels at varying subsampling levels. Further CCP iterations did not provide any noticeable benefit when OOD data was present at the 25% level or beyond. At 100% mismatch, the effect of CCP is not complete immunity, but instead becomes a problem of tuning the subsampling percentage. When no CCP pseudo-labels are kept, the classifier is equivalent to our supervised baseline. At aggressive subsampling values,

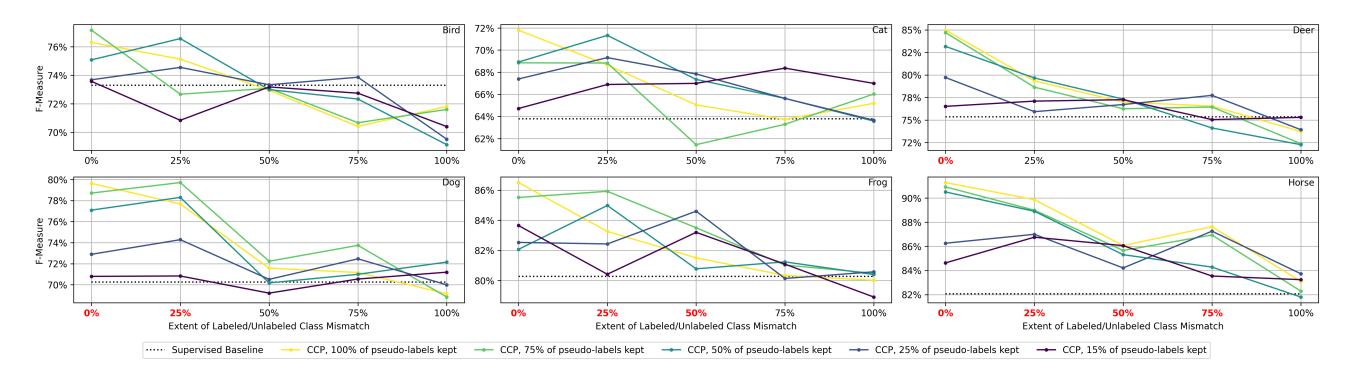


Figure 2: Open-set experiment F-measures. A red x-tick indicates the presence of unlabeled data for that class.

only the OOD samples closest to the in-distribution data remain and the decision boundary is minimally perturbed.

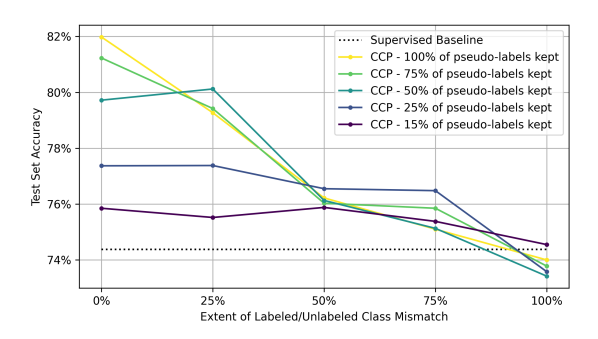


Figure 3: Open-set experiment test set accuracy.

To perform well in these experiments, an algorithm must also be robust to class distribution misalignment as, *e.g.*, the unlabeled data comes from only a single in-distribution class at the 75% mismatch level. In Fig. 2, we show that CCP extracts the new information contained from in-distribution unlabeled data while being robust to OOD data and misalignment. The single class F-measure (Powers, 2011) of the classes in which there were new examples of in the unlabeled data were reliably increased with CCP. If no unlabeled data existed for a class in an experiment, the F-measure is roughly on par with the supervised baseline.

#### 4.4. Noisy-Label Performance

To test the effects of noise in the given labels, we repeated the 0% mismatch environment, but randomly changed a percent of the given labels. The only change we made to Algorithm 1 is that we made the given labels mutable with the same process of pseudo-label proposal and averaging over epochs. In Fig. 4, we can see pseudo-label accuracy substantially improves across 6 iterations for unlabeled and noisy labeled data. In Tab. 2, notably, CCP achieves a higher accuracy than the clean supervised baseline with 30% of its labels randomly changed.

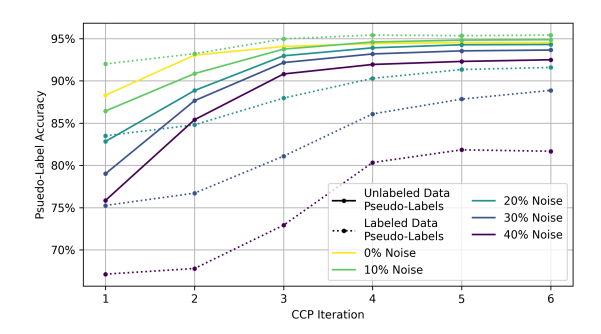


Figure 4: Noisy-label experiment CCP iterations.

Algorithm	Label Noise Percentage						
Aigorithin	0%	10%	20%	30%	40%		
Baseline	74.38%	68.03%	63.37%	56.78%	55.47		
CCP (ours)	83.08%	78.13%	75.72%	75.33%	70.65		

Table 2: Noisy-label experiment test set accuracy.

#### 5. Conclusion

We have presented a novel framework for SSL that combines a novel contrastive approach to pseudo-labeling with an outer iteration designed for learning under label noise. We also introduce a subsampling procedure with a highly generalizable, unsupervised metric to control its effectiveness and provide insight into its effect. The result is a highly reliable and effective SSL framework that does not perform worse than a supervised baseline across four common real-world SSL scenarios including few-label, open-set, noisy-label, and class distribution misalignment. Future work may include augmenting Algorithm 2 to include successful components from related work such as consistency training between weak/strong augmentation (Sohn et al., 2020) and instance/semantic similarity (Zheng et al., 2022).

### References

- Amini, M.-R., Feofanov, V., Pauletto, L., Devijver, E., and Maximov, Y. Self-training: A survey, 2022. URL https://arxiv.org/abs/2202.12040.
- Arazo, E., Ortego, D., Albert, P., O'Connor, N. E., and McGuinness, K. Pseudo-labeling and confirmation bias in deep semi-supervised learning. In *2020 International Joint Conference on Neural Networks (IJCNN)*, pp. 1–8, 2020. doi: 10.1109/IJCNN48605.2020.9207304.
- Berthelot, D., Carlini, N., Cubuk, E. D., Kurakin, A., Sohn, K., Zhang, H., and Raffel, C. Remixmatch: Semi-supervised learning with distribution alignment and augmentation anchoring. *CoRR*, abs/1911.09785, 2019a. URL http://arxiv.org/abs/1911.09785.
- Berthelot, D., Carlini, N., Goodfellow, I., Oliver, A., Papernot, N., and Raffel, C. *MixMatch: A Holistic Approach to Semi-Supervised Learning*. Curran Associates Inc., Red Hook, NY, USA, 2019b.
- Bhattacharjee, A., Karami, M., and Liu, H. Text transformations in contrastive self-supervised learning: A review, 2022. URL https://arxiv.org/abs/2203.12000.
- Cer, D., Yang, Y., Kong, S.-y., Hua, N., Limtiaco, N., John, R. S., Constant, N., Guajardo-Cespedes, M., Yuan, S., Tar, C., Sung, Y.-H., Strope, B., and Kurzweil, R. Universal sentence encoder, 2018. URL https://arxiv.org/abs/1803.11175.
- Chang, M.-W., Ratinov, L., Roth, D., and Srikumar, V. Importance of semantic representation: Dataless classification. In *Proceedings of the 23rd National Conference on Artificial Intelligence Volume 2*, AAAI'08, pp. 830–835. AAAI Press, 2008. ISBN 9781577353683.
- Chapelle, O., Schölkopf, B., and Zien, A. (eds.). Semi-Supervised Learning. The MIT Press, 2006. ISBN 9780262033589. URL http://dblp.uni-trier.de/db/books/collections/CSZ2006.html.
- Chen, B., Jiang, J., Wang, X., Wan, P., Wang, J., and Long, M. Debiased self-training for semi-supervised learning, 2022. URL https://arxiv.org/abs/2202.07136.
- Chen, P., Ye, J., Chen, G., Zhao, J., and Heng, P.-A. Beyond class-conditional assumption: A primary attempt to combat instance-dependent label noise. In *AAAI*, 2021.
- Chen, T., Kornblith, S., Norouzi, M., and Hinton, G. A simple framework for contrastive learning of visual representations. In III, H. D. and Singh, A. (eds.), *Proceedings of the 37th International Conference on Ma-*

- chine Learning, volume 119 of Proceedings of Machine Learning Research, pp. 1597–1607. PMLR, 13–18 Jul 2020a. URL https://proceedings.mlr.press/v119/chen20j.html.
- Chen, T., Kornblith, S., Swersky, K., Norouzi, M., and Hinton, G. Big self-supervised models are strong semi-supervised learners, 2020b. URL https://arxiv.org/abs/2006.10029.
- Chin, J. H. and Ratnavelu, K. A semi-synchronous label propagation algorithm with constraints for community detection in complex networks. *Scientific Reports*, 7, 2017.
- Csiszar, I. *I*-Divergence Geometry of Probability Distributions and Minimization Problems. *The Annals of Probability*, 3(1):146 158, 1975. doi: 10.1214/aop/1176996454. URL https://doi.org/10.1214/aop/1176996454.
- de Carvalho, O. L. F., de Carvalho Junior, O. A., de Albuquerque, A. O., Santana, N. C., Guimaraes, R. F., Gomes, R. A. T., and Borges, D. L. Bounding boxfree instance segmentation using semi-supervised iterative learning for vehicle detection. *IEEE Journal of Selected Topics in Applied Earth Observations and Remote Sensing*, 15:3403–3420, 2022. doi: 10.1109/jstars.2022.3169128. URL https://doi.org/10.1109%2Fjstars.2022.3169128.
- Ding, Y., Zhang, X., Li, B., Xing, J., Qiang, Q., Qi, Z., Guo, M., Jia, S., and Wang, H. Malware classification based on semi-supervised learning. In Su, C., Sakurai, K., and Liu, F. (eds.), *Science of Cyber Security*, pp. 287–301, Cham, 2022. Springer International Publishing. ISBN 978-3-031-17551-0.
- Dong, C. and Schäfer, U. Ensemble-style self-training on citation classification. In *Proceedings of 5th International Joint Conference on Natural Language Processing*, pp. 623–631, Chiang Mai, Thailand, November 2011. Asian Federation of Natural Language Processing. URL https://aclanthology.org/I11-1070.
- Dong, Y., Chen, W., Zhao, H., Ma, X., Gao, T., and Li, X. Label propagation algorithm based on roll-back detection and credibility assessment. *Mathematical Biosciences and Engineering*, 17(3):2432–2450, 2020. ISSN 1551-0018. doi: 10.3934/mbe.2020132. URL https://www.aimspress.com/article/doi/10.3934/mbe.2020132.
- Dwork, C. The promise of differential privacy: A tutorial on algorithmic techniques. In 2011 IEEE 52nd Annual Symposium on Foundations of Computer Science, pp. 1–2, 2011. doi: 10.1109/FOCS.2011.88.

- Gao, S., Wang, Q., and Sun, Y. S2g2: Semi-supervised semantic bird-eye-view grid-map generation using a monocular camera for autonomous driving. *IEEE Robotics and Automation Letters*, 7(4):11974–11981, 2022. doi: 10.1109/LRA.2022.3208377.
- Ghosh, A. and Lan, A. Contrastive learning improves model robustness under label noise. In 2021 IEEE/CVF Conference on Computer Vision and Pattern Recognition Workshops (CVPRW), pp. 2697–2702, 2021. doi: 10.1109/CVPRW53098.2021.00304.
- Heinzerling, B. and Strube, M. BPEmb: Tokenization-free Pre-trained Subword Embeddings in 275 Languages. In chair), N. C. C., Choukri, K., Cieri, C., Declerck, T., Goggi, S., Hasida, K., Isahara, H., Maegaard, B., Mariani, J., Mazo, H., Moreno, A., Odijk, J., Piperidis, S., and Tokunaga, T. (eds.), *Proceedings of the Eleventh International Conference on Language Resources and Evaluation (LREC 2018)*, Miyazaki, Japan, May 7-12, 2018 2018. European Language Resources Association (ELRA). ISBN 979-10-95546-00-9.
- Hendrycks, D. and Gimpel, K. Gaussian Error Linear Units (GELUs). 2016.
- Iscen, A., Tolias, G., Avrithis, Y., and Chum, O. Label propagation for deep semi-supervised learning. In *Proceedings* of the IEEE/CVF Conference on Computer Vision and Pattern Recognition, pp. 5070–5079, 2019.
- Johnson, R. and Zhang, T. Semi-supervised convolutional neural networks for text categorization via region embedding. In Cortes, C., Lawrence, N. D., Lee, D. D., Sugiyama, M., and Garnett, R. (eds.), Advances in Neural Information Processing Systems 28, pp. 919–927. Curran Associates, Inc., 2015.
- Kamnitsas, K., Castro, D., Folgoc, L. L., Walker, I., Tanno, R., Rueckert, D., Glocker, B., Criminisi, A., and Nori, A. Semi-supervised learning via compact latent space clustering. In Dy, J. and Krause, A. (eds.), *Proceedings of the 35th International Conference on Machine Learning*, volume 80 of *Proceedings of Machine Learning Research*, pp. 2459–2468. PMLR, 10–15 Jul 2018. URL https://proceedings.mlr.press/v80/kamnitsas18a.html.
- Khosla, P., Teterwak, P., Wang, C., Sarna, A., Tian, Y., Isola, P., Maschinot, A., Liu, C., and Krishnan, D. Supervised contrastive learning, 2020. URL https://arxiv.org/abs/2004.11362.
- Kim, Y. Convolutional neural networks for sentence classification. In *Proceedings of the 2014 Conference on Empirical Methods in Natural Language Processing, EMNLP* 2014, October 25-29, 2014, Doha, Qatar, A meeting of

- SIGDAT, a Special Interest Group of the ACL, pp. 1746–1751, 2014.
- Kingma, D. P. and Ba, J. Adam: A method for stochastic optimization. *CoRR*, abs/1412.6980, 2015.
- Krizhevsky, A. and Hinton, G. Learning multiple layers of features from tiny images. *Master's thesis, Department of Computer Science, University of Toronto*, 2009.
- Kutt, B., Hewlett, W., Starov, O., and Zhou, Y. Innocent until proven guilty (iupg): Building deep learning models with embedded robustness to out-of-distribution content. In 2021 IEEE Security and Privacy Workshops (SPW), pp. 49–55, 2021. doi: 10.1109/SPW53761.2021.00016.
- Lee, D.-H. et al. Pseudo-label: The simple and efficient semi-supervised learning method for deep neural networks. In *Workshop on challenges in representation learning, ICML*, volume 3, pp. 896, 2013.
- Lehmann, J., Isele, R., Jakob, M., Jentzsch, A., Kontokostas, D., Mendes, P., Hellmann, S., Morsey, M., Van Kleef, P., Auer, S., and Bizer, C. Dbpedia a large-scale, multilingual knowledge base extracted from wikipedia. *Semantic Web Journal*, 6, 01 2014. doi: 10.3233/SW-140134.
- Li, H., Zhang, R., Zhao, Z., and Liu, X. Lpa-mni: An improved label propagation algorithm based on modularity and node importance for community detection. *Entropy*, 23:497, 04 2021a. doi: 10.3390/e23050497.
- Li, J., Xiong, C., and Hoi, S. C. H. Comatch: Semisupervised learning with contrastive graph regularization. 2021 IEEE/CVF International Conference on Computer Vision (ICCV), pp. 9455–9464, 2021b.
- Li, P.-Z., Huang, L., Wang, C.-D., Lai, J.-H., and Huang, D. Community detection by motif-aware label propagation. *ACM Trans. Knowl. Discov. Data*, 14(2), feb 2020. ISSN 1556-4681. doi: 10.1145/3378537. URL https://doi.org/10.1145/3378537.
- Liu, J., Song, H., and Wang, J. Open-set fault diagnosis method for industrial process based on semi-supervised learning. In Liu, H., Yin, Z., Liu, L., Jiang, L., Gu, G., Wu, X., and Ren, W. (eds.), *Intelligent Robotics and Applications*, pp. 103–112, Cham, 2022. Springer International Publishing. ISBN 978-3-031-13841-6.
- Loshchilov, I. and Hutter, F. SGDR: stochastic gradient descent with warm restarts. In 5th International Conference on Learning Representations, ICLR 2017, Toulon, France, April 24-26, 2017, Conference Track Proceedings. OpenReview.net, 2017. URL https://openreview.net/forum?id=Skq89Scxx.

- Lugo, G., Hajari, N., and Cheng, I. Semi-supervised learning approach for localization and pose estimation of texture-less objects in cluttered scenes. *Array*, pp. 100247, 2022.
- Malhotra, D. and Chug, A. A modified label propagation algorithm for community detection in attributed networks. *International Journal of Information Management Data Insights*, 1(2):100030, 2021. ISSN 2667-0968. doi: https://doi.org/10.1016/j.jjimei.2021.100030. URL https://www.sciencedirect.com/science/article/pii/S2667096821000239.
- Oh, Y., Kim, D., and Kweon, I. S. Distribution-aware semantics-oriented pseudo-label for imbalanced semi-supervised learning. *CoRR*, abs/2106.05682, 2021. URL https://arxiv.org/abs/2106.05682.
- Oliver, A., Odena, A., Raffel, C. A., Cubuk, E. D., and Goodfellow, I. Realistic evaluation of deep semi-supervised learning algorithms. In Bengio, S., Wallach, H., Larochelle, H., Grauman, K., Cesa-Bianchi, N., and Garnett, R. (eds.), *Advances in Neural Information Processing Systems*, volume 31. Curran Associates, Inc., 2018. URL https://proceedings.neurips.cc/paper/2018/file/c1fea270c48e8079d8ddf7d06d26ab52-Paper.pdf.
- Pang, B. and Lee, L. Seeing stars: Exploiting class relationships for sentiment categorization with respect to rating scales. In *Proceedings of the 43rd Annual Meeting of the Association for Computational Linguistics (ACL'05)*, pp. 115–124, Ann Arbor, Michigan, June 2005. Association for Computational Linguistics. doi: 10.3115/1219840.1219855. URL https://aclanthology.org/P05-1015.
- Polyak, B. Some methods of speeding up the convergence of iteration methods. *Ussr Computational Mathematics and Mathematical Physics*, 4:1–17, 1964.
- Powers, D. M. W. Evaluation: From precision, recall and f-measure to roc., informedness, markedness & correlation. *Journal of Machine Learning Technologies*, 2(1):37–63, 2011.
- Sahito, A., Frank, E., and Pfahringer, B. Better self-training for image classification through self-supervision, 2021. URL https://arxiv.org/abs/2109.00778.
- Shi, W., Gong, Y., Ding, C., Tao, Z. M., and Zheng, N. Transductive semi-supervised deep learning using minmax features. In *Proceedings of the European Conference on Computer Vision (ECCV)*, pp. 299–315, 2018.

- Sohn, K., Berthelot, D., Carlini, N., Zhang, Z., Zhang, H., Raffel, C. A., Cubuk, E. D., Kurakin, A., and Li, C.-L. Fixmatch: Simplifying semi-supervised learning with consistency and confidence. In Larochelle, H., Ranzato, M., Hadsell, R., Balcan, M., and Lin, H. (eds.), *Advances in Neural Information Processing Systems*, volume 33, pp. 596–608. Curran Associates, Inc., 2020. URL https://proceedings.neurips.cc/paper/2020/file/06964dce9addb1c5cb5d6e3d9838f733-Paper.pdf.
- Song, H., Kim, M., Park, D., and Lee, J. Learning from noisy labels with deep neural networks: A survey. *CoRR*, abs/2007.08199, 2020. URL https://arxiv.org/abs/2007.08199.
- Sutskever, I., Martens, J., Dahl, G., and Hinton, G. On the importance of initialization and momentum in deep learning. In Dasgupta, S. and McAllester, D. (eds.), *Proceedings of the 30th International Conference on Machine Learning*, volume 28 of *Proceedings of Machine Learning Research*, pp. 1139–1147, Atlanta, Georgia, USA, 17–19 Jun 2013. PMLR. URL https://proceedings.mlr.press/v28/sutskever13.html.
- Wang, D., Zhang, Y., Zhang, K., and Wang, L. Focalmix: Semi-supervised learning for 3d medical image detection. In *Proceedings of the IEEE/CVF Conference on* Computer Vision and Pattern Recognition (CVPR), June 2020.
- Wang, G.-H. and Wu, J. R2-d2: Repetitive reprediction deep decipher for semi-supervised deep learning. *arXiv* preprint arXiv:2202.08955, 2022.
- Wang, Q., Li, W., and Gool, L. V. Semi-supervised learning by augmented distribution alignment. *CoRR*, abs/1905.08171, 2019. URL http://arxiv.org/abs/1905.08171.
- Xie, J., Szymanski, B. K., and Liu, X. Slpa: Uncovering overlapping communities in social networks via a speaker-listener interaction dynamic process. In 2011 IEEE 11th International Conference on Data Mining Workshops, pp. 344–349, 2011. doi: 10.1109/ICDMW.2011.154.
- Xie, Q., Dai, Z., Hovy, E., Luong, M.-T., and Le, Q. V. Unsupervised data augmentation for consistency training, 2020a.
- Xie, Q., Luong, M.-T., Hovy, E., and Le, Q. V. Self-training with noisy student improves imagenet classification. In 2020 IEEE/CVF Conference on Computer Vision and Pattern Recognition (CVPR), pp. 10684–10695, 2020b. doi: 10.1109/CVPR42600.2020.01070.

- Yang, X., Song, Z., King, I., and Xu, Z. A survey on deep semi-supervised learning. *CoRR*, abs/2103.00550, 2021. URL https://arxiv.org/abs/2103.00550.
- Zagoruyko, S. and Komodakis, N. Wide residual networks. *CoRR*, abs/1605.07146, 2016. URL http://arxiv.org/abs/1605.07146.
- Zhang, X., Zhao, J. J., and LeCun, Y. Character-level convolutional networks for text classification. *CoRR*, abs/1509.01626, 2015. URL http://arxiv.org/abs/1509.01626.
- Zhang, Y., Zhang, X., Qiu, R. C., Li, J., Xu, H., and Tian, Q. Semi-supervised contrastive learning with similarity co-calibration. *ArXiv*, abs/2105.07387, 2022.
- Zheng, M., You, S., Huang, L., Wang, F., Qian, C., and Xu, C. Simmatch: Semi-supervised learning with similarity matching. In 2022 IEEE/CVF Conference on Computer Vision and Pattern Recognition (CVPR), pp. 14451–14461, Los Alamitos, CA, USA, jun 2022. IEEE Computer Society. doi: 10.1109/CVPR52688.2022.01407. URL https://doi.ieeecomputersociety.org/10.1109/CVPR52688.2022.01407.
- Zhou, Y., Yang, L., and Cao, Y. Semi-supervised false data injection attacks detection in smart grid. In Lin, J. and Tang, Q. (eds.), *Applied Cryptography in Computer and Communications*, pp. 189–200, Cham, 2022. Springer Nature Switzerland. ISBN 978-3-031-17081-2.
- Zhu, X. and Ghahramani, Z. Learning from labeled and unlabeled data with label propagation. 2002.

## A. Additional Illustrations

Refer to Fig. 5 for an illustrated depiction of how  $f_b$ ,  $f_z$ , and  $f_g$  are organized using the CCP framework. Fig. 6 provides a concrete example of a credibility vector calculation, how it differs from a traditional label vector, and the effect on a cross-entropy calculation.

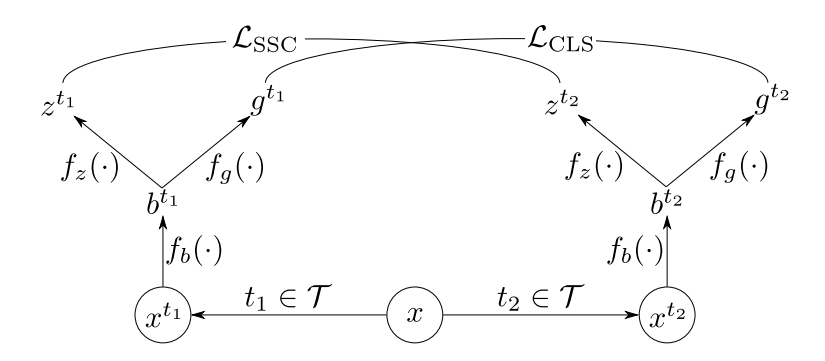


Figure 5: CCP uses an encoder  $f_b(\cdot)$  and two projection heads:  $f_z(f_b(\cdot))$  for contrastive credibility propagation and  $f_g(f_b(\cdot))$  for classification.

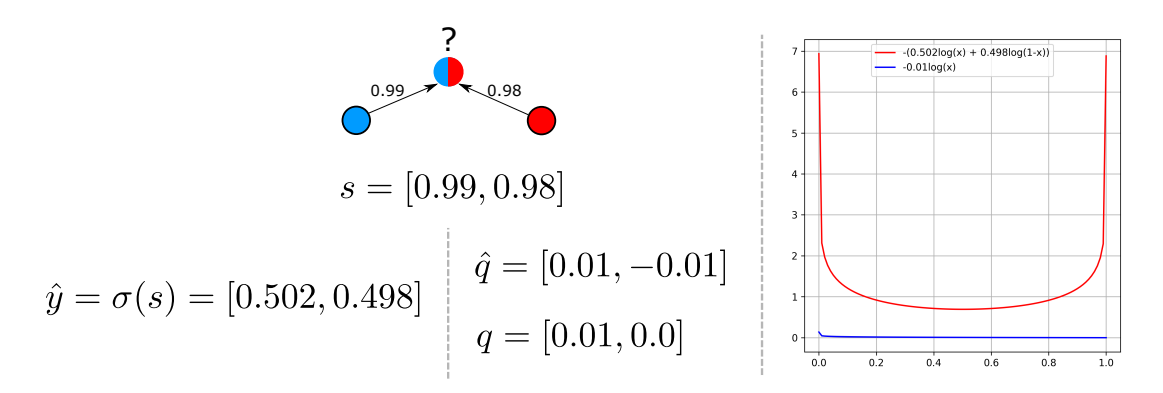


Figure 6: Left: In this example, an unlabeled sample is highly similar to the blue and red classes with similarity scores of 0.99 and 0.98, respectively. A traditional label vector,  $\hat{y}$ , will be computed as a softmax across these similarity scores. The credibility vector,  $\hat{q}$ , is computed with 0.99-0.98=0.01 in the first entry and 0.98-0.99=-0.01 in the second.  $\hat{q}$  is then clipped to a range of [0,1]. Right: A cross-entropy calculation supervised with  $\hat{y}$  and q differ greatly. Consider x to be the softmax output of a classifier for the blue class. Using  $\hat{y}$  to compute cross-entropy will induce a strong gradient at either pole despite that the true class of the unlabeled sample is very nearly ambiguous. Using q will ensure the loss for this sample is near zero regardless of what x is except for a small gradient near x=0 since there is some minor evidence that the true class of the unlabeled sample is blue.

## **B.** Dataset Details

Summary details on the classification datasets used in this work are displayed in Tab. 3.

# C. CCP Iteration Performance

In Tab. 4 we display the accuracy of pseudo-labels produced by CCP at each iteration with and without subsampling at all levels of label availability for every text dataset: Our DLP dataset, AG News (Zhang et al., 2015), DBpedia (Zhang et al., 2015; Lehmann et al., 2014), Rotten Tomatoes (Pang & Lee, 2005), and Yahoo! Answers (Chang et al., 2008; Zhang et al., 2015). We can see most runs have converged after seven iterations although minor improvements are still occurring in some runs. Using subsampling can occasionally decrease performance across iterations *e.g.* on the Rotten Tomatoes dataset at

Dataset	No. Classes	Balanced	No. Train Samples	Classification Task
DLP	8	No	559,141	Sensitivity + Category
AG News	4	Yes	120,000	Topic
DBpedia	14	Yes	560,000	Topic
Rotten Tomatoes	2	No	271,772	Sentiment
Yahoo! Answers	10	Yes	700,000	Topic
CIFAR-10	10	Yes	50,000	Image Subject

Table 3: Description of each benchmark dataset.

0.1% label availability. After seven iterations, the accuracy is higher than when not using subsampling, but further iterations appear to be decreasing accuracy. This necessitates the careful tuning of a subsampling schedule. Also, occasionally, runs without subsampling appear to return a higher accuracy at termination by a small margin despite a slower start. Again, this is explainable by an accumulation of errors brought forth by subsampling. A smaller initial  $d_{\text{max}}$  would alleviate this situation. We use  $\Xi=40$  in each CCP iteration for every text dataset. This means all eight CCP iterations consisted of only 320 epochs which are smaller than a typical supervised training session. However, if more epochs are used per iteration, CCP can introduce more significant costs compared to a typical supervised training session.

Fig. 7 details the pseudo-label accuracy across CCP iterations when using the CIFAR-10 (Krizhevsky & Hinton, 2009) dataset. Fig. 7 also depicts the possible benefit of resetting  $d_{\rm max}$  back to its original value of 0.01 in certain situations. In general, there is a benefit to doing this when the state of pseudo-labels has converged yet there still exists considerable errors and weak predictions. This can be seen by the large boost in pseudo-label accuracy after resetting  $d_{\rm max}$  in the 40-label scenario when the pseudo-label error is highest. The benefit in the 250-label scenario is less pronounced. There is no benefit to resetting  $d_{\rm max}$  in the 4000-label scenario. In this scenario, you're resetting many pseudo-labels that were already correct and it takes several additional iterations for the overall pseudo-label accuracy to recover. However, a smaller value for  $d_{\rm max}$  in the 4000-label experiment may still have provided benefit. In the 40-label experiment, pseudo-label accuracy still has a considerable upward trajectory after 18 iterations. In general, a larger number of clean labels ensures CCP converges more quickly. Also, more aggressive subsampling schedules provide stronger benefits when the error in the pseudo-labels is higher e.g. when given labels are few.

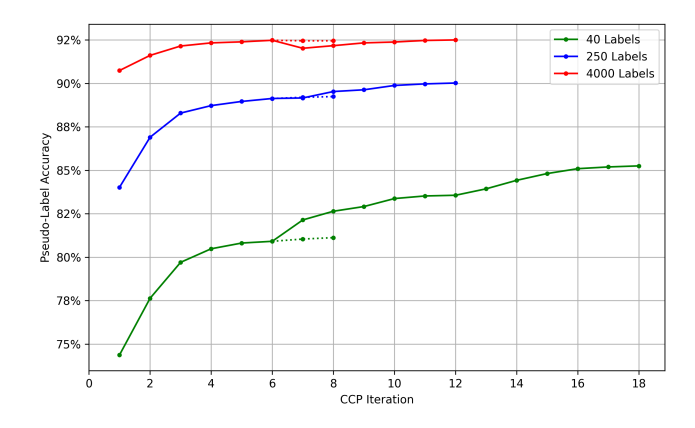


Figure 7: Pseudo-label accuracy across CCP iterations with the CIFAR-10 dataset. The subsampling schedule is set with the standard values of  $d_{\rm max}=0.01$  with a divisor of 10 after each CCP iteration. In the solid lines, the value of  $d_{\rm max}$  is reset back to 0.01 after every 6 iterations. The dotted lines represent the pseudo-label accuracy obtained without resetting  $d_{\rm max}$ .

# D. Subsampling Pseudo-Labels

In Fig. 8, we observe that subsampling based on  $\{\hat{\omega}_u\}_{u\in U}$  helps to isolate correct pseudo-labels across all text datasets. We can see this is due to correctly propagated labels having considerably stronger confidence than incorrect ones. "Easy" unlabeled samples, *i.e.* samples with high similarity to a labeled sample, are more likely to be predicted correctly with a

strong credibility value. "Hard" samples will have weak credibility scores and are more likely to be incorrect.

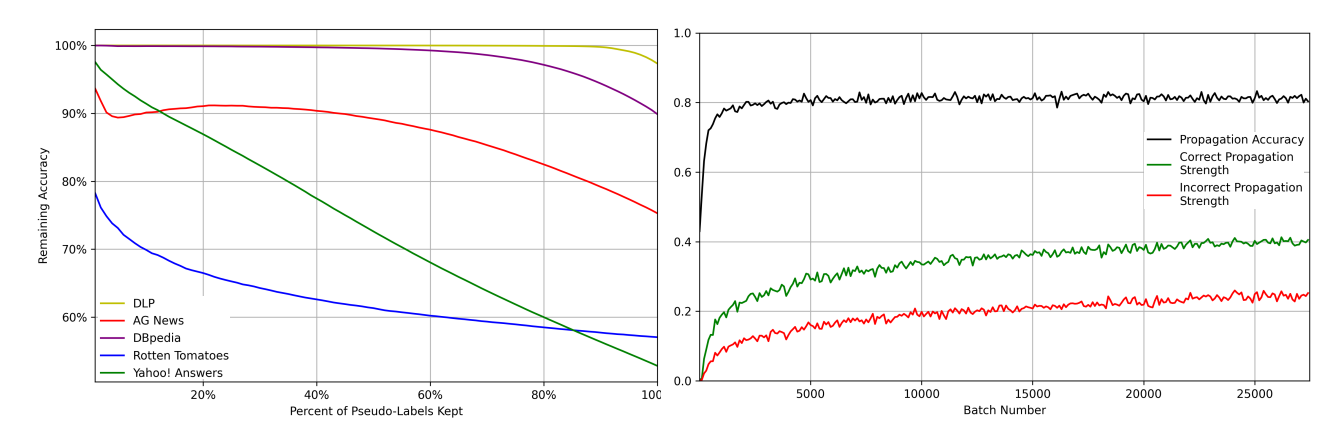


Figure 8: Left: The accuracy among the remaining  $\{q_u\}_{u\in U}$  after one iteration of CCP at different p levels. Right: Exponential moving averages over 40 epochs of the batch propagation accuracy and  $\hat{\omega}$  of correct and incorrect pseudo-labels for the DLP dataset.

In Figs. 9 to 13, for each text dataset, we vary the number of pseudo-labels kept (1-p) while comparing the resulting KL-Divergence (as defined in Algorithm 3) and the resulting classifier accuracy when trained on the subsampled pseudo-labels. All classifiers, and the model which produced the initial pseudo-labels, had access to 0.1% of labels.

The most frequent observation is a small increase in classifier accuracy at approximately  $d_{\rm max}=0.01$  and a drop off in accuracy as  $d_{\rm max}$  becomes too large. The only exception is on the Rotten Tomatoes dataset where large values of  $d_{\rm max}=0.01$  appear to continue to increase the resulting classifier accuracy. The Rotten Tomatoes dataset is the dataset in which our baseline model performs the worst – only slightly better than random guessing. This would suggest that one would need more aggressive values of p to achieve accuracy increases. This is evidenced in our main results also where increasing p results in the slowest increase in accuracy for Rotten Tomatoes compared to all other datasets. In general, this suggests that more aggressive values for  $d_{\rm max}$  should be chosen when the baseline model performance is worse, but this requires further investigation.

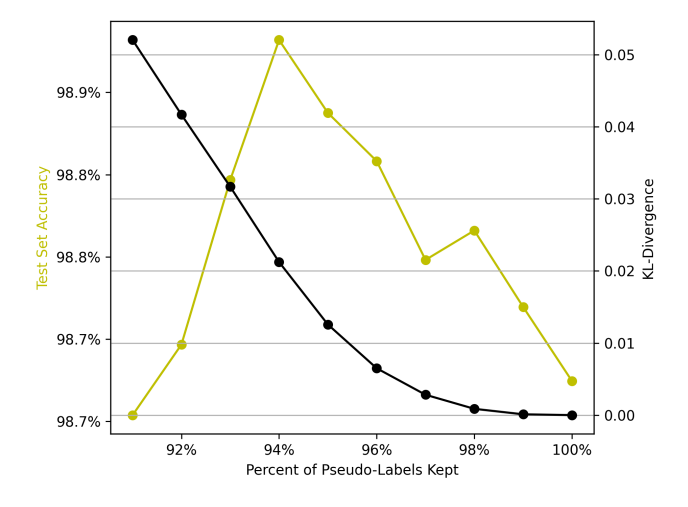


Figure 9: KL-Divergence vs Accuracy at varying levels of 1-p with the DLP dataset.

# E. Toggling Transformations in CCP

In Fig. 14, we consider the effect of turning transformations off in CCP. We first gather all the pseudo-labels produced by CCP on the DLP dataset after a single iteration with and without transformations at all levels of label availability. We then

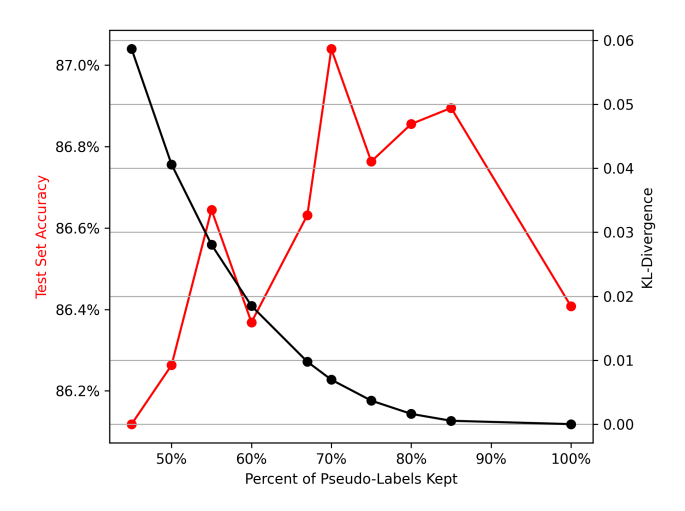


Figure 10: KL-Divergence vs Accuracy at varying levels of 1 - p with the AG News dataset.

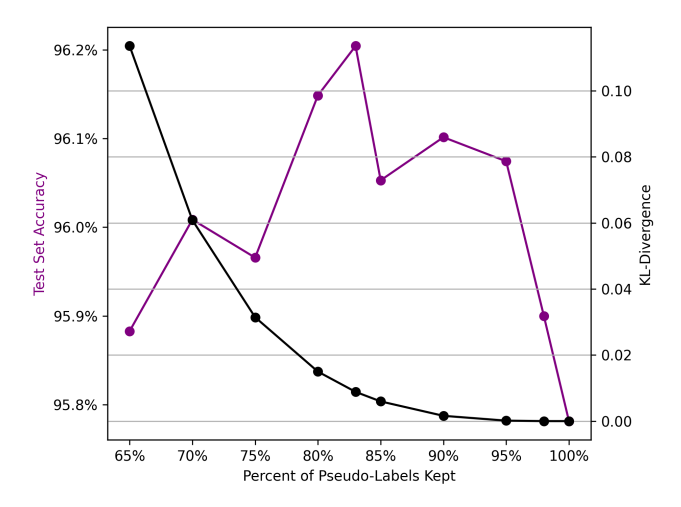


Figure 11: KL-Divergence vs Accuracy at varying levels of 1-p with the DBpedia dataset.

subsample the pseudo-labels with our proposed subsampling procedure at all levels of p and compare the resulting accuracy of the subsample. It is clear to see using transformations has a large impact on subsample accuracy at all levels of p and label availability. The effect is more pronounced as label availability becomes scarce.

## F. Details on Transformations

Each transformation used in this work features one or more parameters that control the magnitude of its effect. Along with the transformation type, these parameters are randomly varied during training within predefined bounds. For efficiency, two text transformations are randomly drawn per forward pass and applied to each image with random parameters to form two transformed batches. For images, to closely match the experiments of other work, all transformations are applied sequentially per image with a probability of occurring. Random crop, horizontal flip, color jitter, and grayscale transformation occurs with probability 100%, 50%, 80%, 20%, respectively. A description of each  $t \in \mathcal{T}$  can be found below.

#### • Text transformations:

- **Differential Privacy**: Laplacian noise is applied to all EVs in a fashion that is common in the practice of Differential Privacy (Dwork, 2011). We randomly vary the strength of the noise,  $\epsilon$ , between 10 and 100.
- Gaussian Noise: Gaussian noise is applied to all EVs. We randomly vary  $\mu$  and sigma between [-0.5, 0.5] and

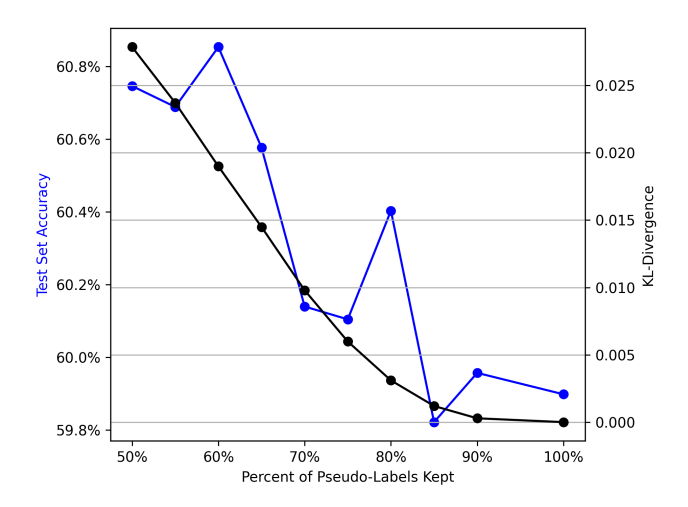


Figure 12: KL-Divergence vs Accuracy at varying levels of 1-p with the Rotten Tomatoes dataset.

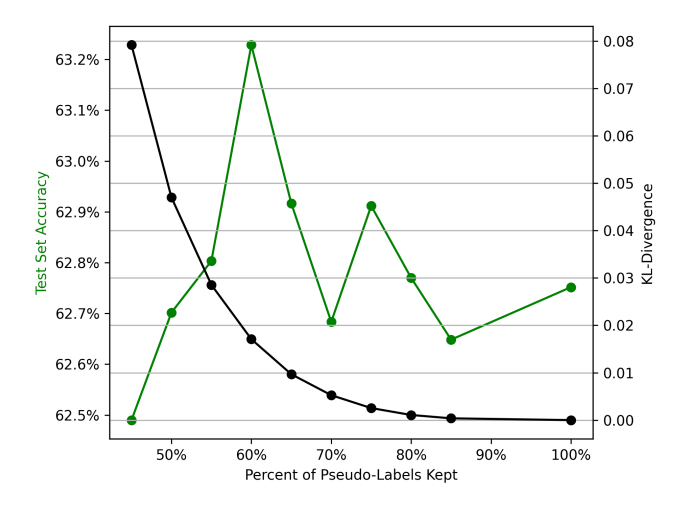


Figure 13: KL-Divergence vs Accuracy at varying levels of 1-p with the Yahoo! Answers dataset.

[0.01, 0.05], respectively.

- Vector Hide: We randomly replace EVs with the learned padding vector used to pad short inputs. The amount of EVs replaced is randomly varied from 10% to 25% of the total length.
- Paragraph Swap: We choose a random index along the length of a sequence of EVs and swap the content above and below that index.
- Random Vector Swap: We randomly replace EVs with randomly chosen EVs from the full vocabulary. The amount of EVs replaced is randomly varied from 10% to 25% of the total length.
- Scramble: We randomly select indices across the length of a sequence of EVs and randomly scramble their order. The amount of EVs we choose to scramble randomly varies from 10% to 25% of the total length.

# • Image transformations:

- Random crop: Take a random crop of the image containing, at a minimum, 10% of the original image. Given that the aspect ratio (width over height) of CIFAR-10 images is 1.0, The aspect ratio of the crop must fall within [0.75, 1.25]. The image crops are resized back to 32 × 32 using bicubic interpolation.
- Horizontal flip: Flip images left-to-right.
- Color Jitter: Randomly distort the brightness, contrast, saturation, and hue of an image in a randomly chosen order. The maximum delta for brightness, contrast, and saturation jitter is set to 0.72 and 0.18 for hue jitter.

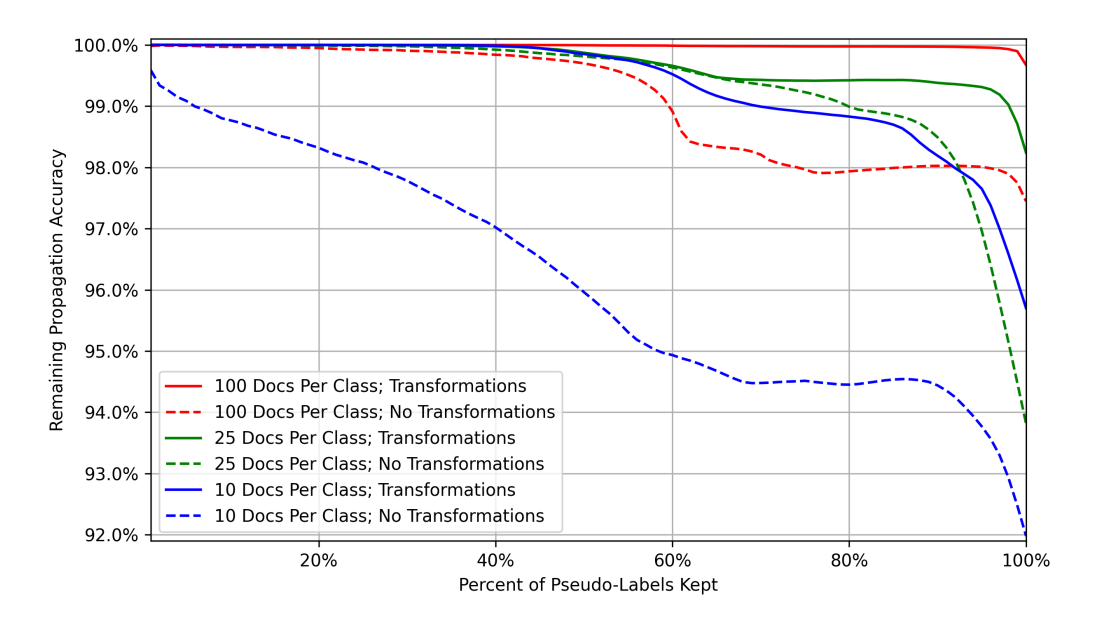


Figure 14: Subsample pseudo-label accuracy while toggling the use of transformations on the DLP dataset at all levels of p and label availability.

- **Grayscale**: Transform the colors of the entire image to grayscale.

# **G.** Additional Training Details

For text data, we use the BPEmb byte-pair encoder (Heinzerling & Strube, 2018) to transform a text document into a sequence of token indices cropped to a certain size. Each token index is used to look up an embedding vector (EV) whose initial values are set to the pretrained BPEmb values. The sequence of EVs is read by parallel convolutional layers whose output then feeds into additional convolutional layers depth-wise. The final activation maps undergo global max pooling to obtain a single floating point value per filter. These maximum activations are concatenated together to form  $b_i$ .  $f_z$  and  $f_g$  are designed as a 2-layer MLP. For  $f_z$ , the size of the hidden (output) layer is 64 (32). For  $f_g$  the hidden layer is of size 64 and the output layer size is the number of classes. Small adjustments are made to  $f_b$  to ensure the control and baseline reached the desired performance on each text dataset. An illustration of  $f_b$  used for text datasets can be found in Fig. 16. More information about the hyperparameters of  $f_b$  for each dataset can be found in Tab. 5.

For CIFAR-10, we adopt WRN28-2 (Zagoruyko & Komodakis, 2016). We use a standard SGD optimizer with Nesterov momentum (Polyak, 1964; Sutskever et al., 2013). We use a cosine learning rate decay (Loshchilov & Hutter, 2017). The learning rate is calculated as  $0.03\cos(\frac{7\pi s}{16S})$  where s is the current training step, and S is the total number of training steps. Each CCP iteration is allowed to continue until convergence of  $\mathcal{L}_{SSC}$  as measured with an exponential moving average of each batch loss. When building classifiers, we use a fixed length of 1000 epochs. We do not use an exponential moving average of hyperparameters. This, along with other configurations not reported in prior work, may account for some differences in our control performance compared to them.

# H. Pseudo-Label Oscillation

In a similar fashion to (Chen et al., 2021), we observe oscillations of the predicted pseudo-label across epochs in the presence of a pseudo-label error. The credibility vector value for the correct class begins high (or at least reflects uncertainty *i.e.* near zero) but the network eventually memorizes the incorrect pseudo-label as training continues. When there is no pseudo-label error, the magnitude of oscillation is significantly less. Oscillations are also observed during the first iteration when no prior pseudo-label exists. This is attributable to the effects of random batch selection and network state. Randomly chosen examples of these behaviors are illustrated in Fig. 17.

This allows us to use a similar theoretical motivation as (Chen et al., 2021) for averaging across an epoch in CCP. Assume

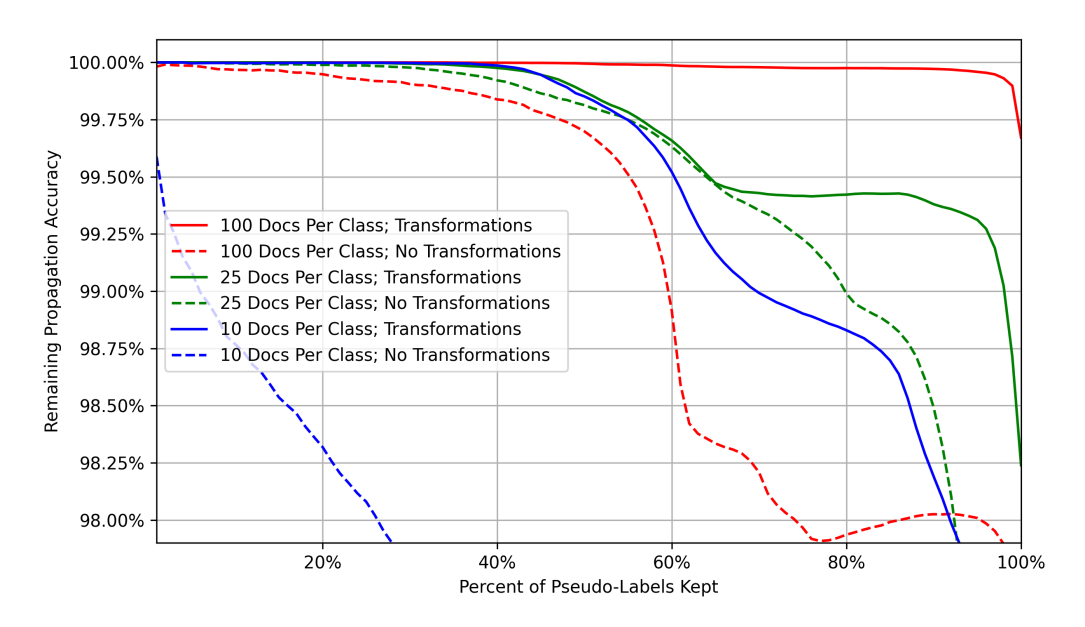


Figure 15: A zoomed-in look into Fig. 14.

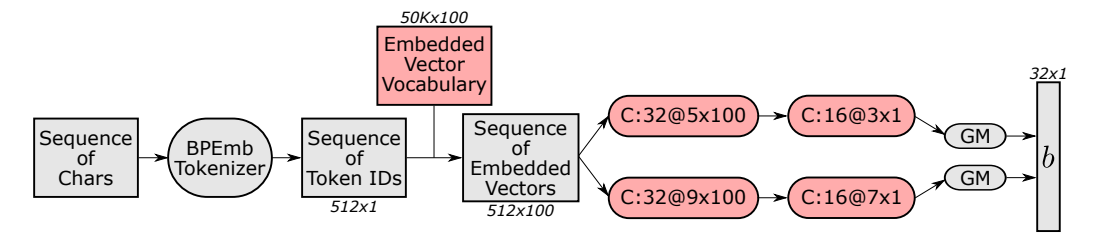


Figure 16: An illustration of an example encoder used in this work,  $f_b$ , for text data. "C:32@5×100" refers to a convolutional layer with 32 filters each of size  $5 \times 100$ . "GM" refers to global max pooling over the feature activation maps. Red indicates learnable variables.

there is a latent optimal pseudo-label for an unlabeled sample  $x_u$  denoted  $q_u^* \in \mathbb{R}^K$ . Denote the pseudo-label obtained at the end of CCP iteration m as  $q_u^{[\cdot,m]}$ . Based on the oscillatory behavior of pseudo-labels, we can approximate the pseudo-label at the  $\xi$ -th epoch of the m-th iteration for  $m \geq 1$ , denoted  $q_u^{[\xi,m]}$ , as,

$$q_u^{[\xi,m]} \approx \alpha_u^{[\xi,m]} \beta_u^{[\xi,m]} + (1 - \alpha_u^{[\xi,m]}) q_u^{[\cdot,m-1]}$$
(4)

Where  $\xi \in \{1,2,\ldots,\Xi\}$ ,  $q_u^{[\cdot,0]}$  are zero vectors,  $\alpha_u^{[\xi,m]} \in [0,1]$  are coefficients dependent on instances, the network, and  $q_u^{[\cdot,m-1]}$  with  $\alpha_u^{[\xi,1]} = 1 \quad \forall \xi$ , and  $\beta_u^{[\xi,m]} \in \mathbb{R}^K$  are i.i.d. random vectors with  $\mathbb{E}[\beta_u^{[\xi,m]}] = q_u^*$ . Consider a uniformly chosen random epoch and iteration denoted  $\xi'$  and m', respectively. We can see,

$$\|\mathbb{E}[q_u^{[\cdot,m'+1]}] - q_u^*\| \le \|q_u^{[\cdot,m']} - q_u^*\| \tag{5}$$

$$\operatorname{var}(q_{u,k}^{[\cdot,m']}) \le \operatorname{var}(q_{u,k}^{[\xi',m']}) \quad \forall k \in c$$

$$\tag{6}$$

That is, CCP is expected to improve the quality of pseudo-labels iteratively and new pseudo-labels at the end of an iteration have lower variance due to the averaging mechanism.

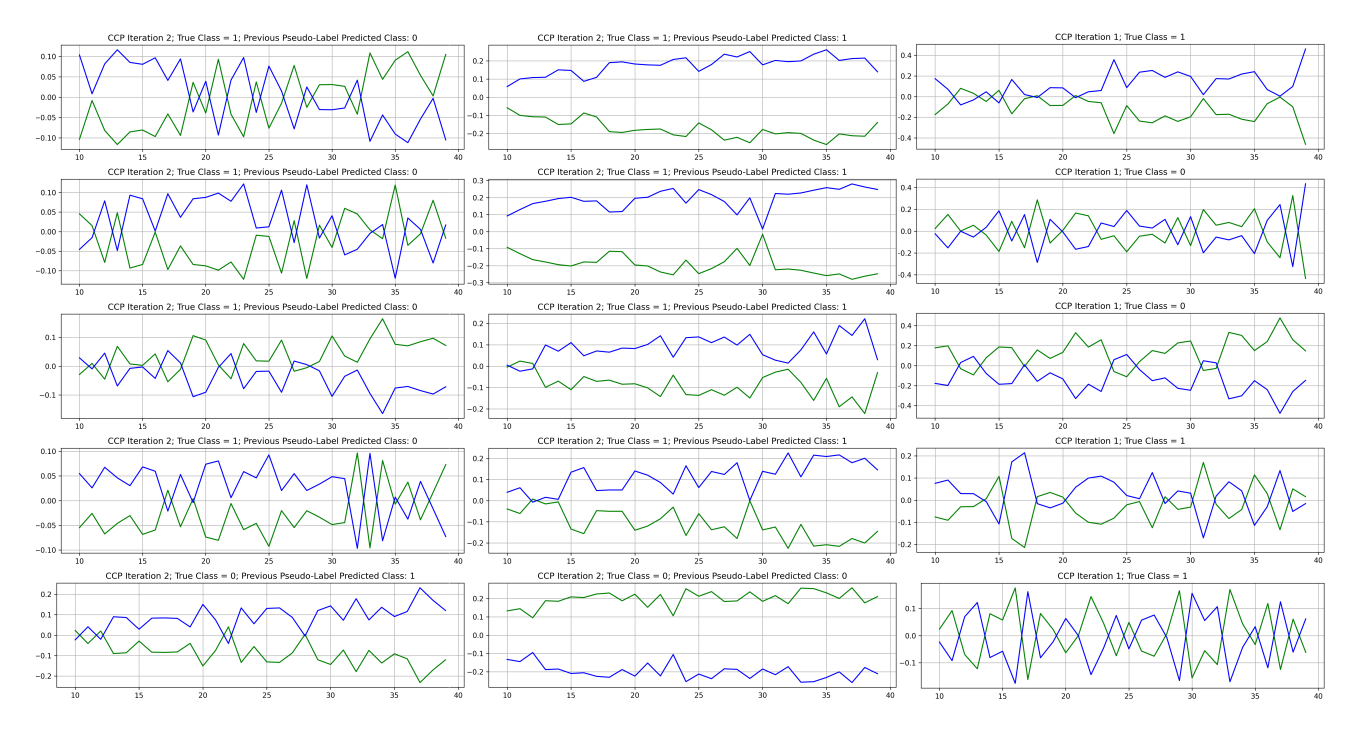


Figure 17: Randomly chosen plots from the Rotten Tomatoes dataset with 1% label availability depicting pseudo-label oscillation over epochs. On the x-axis is the epoch number. On the y-axis is the non-scaled credibility value for class 1 in blue and class 0 in green. The leftmost column shows oscillation in the presence of a pseudo-label error. The middle column displays significantly degraded oscillation in the presence of a correct pseudo-label. The rightmost column depicts oscillations which can also be observed in the first CCP iteration.

	% of Labels	Subsampling	Iteration						
Dataset			1	2	3	4	5	6	7
	1%	N	99.14%	99.40%	99.49%	99.51%	99.54%	99.55%	99.56%
		Y	99.14%	99.46%	99.57%	99.64%	99.66%	99.68%	99.68%
DLP	0.1%	N	97.33%	97.82%	97.98%	98.10%	98.15%	98.19%	98.19%
		Y	97.33%	98.03%	98.34%	98.42%	98.50%	98.54%	98.55%
	0.05%	N	93.87%	94.80%	95.26%	95.59%	95.82%	96.07%	96.24%
		Y	93.87%	95.10%	95.30%	95.36%	95.43%	95.48%	95.53%
	1.07	N	83.51%	86.68%	87.30%	87.60%	87.79%	87.95%	87.89%
	1%	Y	83.51%	86.50%	86.54%	87.23%	87.67%	88.00%	88.13%
AG News	0.107	N	75.29%	81.62%	83.27%	84.03%	84.48%	84.67%	84.84%
	0.1%	Y	75.29%	82.17%	83.37%	84.18%	84.74%	85.15%	85.49%
	0.05%	N	67.14%	76.71%	79.66%	80.78%	81.70%	82.27%	82.72%
		Y	67.14%	77.56%	80.36%	81.56%	82.00%	82.63%	82.98%
	1%	N	96.24%	97.23%	97.55%	97.69%	97.71%	97.78%	97.81%
		Y	96.24%	96.80%	97.06%	97.44%	97.58%	97.66%	97.85%
DBpedia	0.1%	N	89.88%	92.84%	93.79%	94.23%	94.58%	94.81%	94.87%
1		Y	89.88%	93.45%	94.11%	94.42%	94.84%	95.01%	95.25%
	0.05%	N	82.75%	87.43%	89.08%	89.99%	90.57%	90.86%	91.09%
		Y	82.75%	88.17%	90.04%	91.06%	91.50%	91.96%	92.26%
	1%	N	64.29%	67.84%	68.89%	69.42%	69.55%	69.57%	69.70%
		Y	64.29%	68.94%	69.92%	70.46%	70.60%	70.66%	70.61%
Rotten Tomatoes	0.1%	N	57.04%	57.75%	58.17%	58.32%	58.38%	58.44%	58.50%
		Y	57.04%	58.30%	59.11%	59.34%	59.28%	59.22%	59.14%
	0.05%	N	54.75%	55.28%	55.65%	55.79%	55.89%	55.93%	55.96%
		Y	54.75%	55.53%	56.31%	56.41%	56.38%	56.42%	56.41%
	1%	N	63.06%	65.70%	66.46%	66.88%	66.90%	67.13%	67.22%
		Y	63.06%	66.20%	66.43%	66.87%	67.06%	67.30%	67.31%
Yahoo! Answers	0.1%	N	52.82%	58.23%	59.76%	60.53%	60.99%	61.37%	61.61%
		Y	52.82%	58.57%	59.83%	60.32%	60.60%	60.76%	60.92%
	0.050	N	45.25%	52.94%	55.28%	56.45%	57.19%	57.70%	57.99%
	0.05%	Y	45.25%	53.50%	55.89%	56.98%	57.56%	57.89%	58.13%

Table 4: The accuracy of pseudo-labels after seven iterations of CCP. All runs with subsampling uses an initial  $d_{\rm max}=0.01$ .

Hyperparameter	DLP	AG News	DBpedia	Rotten Tomatoes	Yahoo! Answers
Input Size	512	512	512	256	1024
Droput Rate	0.0	0.0	0.0	0.8	0.8
Batch Size	256	256	256	256	256
Optimizer	Adam	Adam	Adam	Adam	Adam
Activation	GELU	GELU	GELU	GELU	GELU
au	0.1	0.1	0.1	0.1	0.1
Ξ	40	40	40	40	40
Weight Decay	0.0	0.0	0.0	0.001	0.001
Learning Rate	0.00004	0.00004	0.00004	0.00004	0.00004
First Sequence of Parallel Convolutional Layers	$32@5 \times 100 \rightarrow 16@3 \times 1$	$32@5 \times 100 \rightarrow 16@3 \times 1$	$32@5{\times}100 \rightarrow 16@3{\times}1$	$32@5 \times 100 \rightarrow 16@3 \times 1$	$64@5 \times 100 \rightarrow 32@3 \times 1$
Second Sequence of Parallel Convolutional Layers	$32@9{\times}100 \rightarrow 16@7{\times}1$	$32@9{\times}100 \rightarrow 16@7{\times}1$	$32@9{\times}100 \rightarrow 16@7{\times}1$	$32@9{\times}100 \rightarrow 16@7{\times}1$	$64@9{\times}100 \rightarrow 32@7{\times}1$
Third Sequence of Parallel Convolutional Layers	-	-	-	-	$64@13 \times 100 \rightarrow 32@9 \times 1$
Global Max Pooling	True	True	True	True	True

Table 5: Hyperparameter settings of  $f_b$  for each text dataset. "32@5×100" refers to a convolutional layer with 32 filters each of size  $5 \times 100$  (Kingma & Ba, 2015; Hendrycks & Gimpel, 2016).